# Observation of Multiple Radical Pair States in Photosystem 2 Reaction Centers†

Paula J. Booth,*,‡ Ben Crystall, Iqbal Ahmad,§ James Barber,∥ George Porter, and David R. Klug
*Photochemistry Research Group, Department of Biology and AFRC Photosynthesis Research Group, Department of Biochemistry, Imperial College, London SW7 2BB, U.K.*

*Received February 27, 1991; Revised Manuscript Received May 8, 1991*

ABSTRACT: Charge recombination of the primary radical pair in D1/D2 reaction centers from photosystem 2 has been studied by time-resolved fluorescence and absorption spectroscopy. The kinetics of the primary radical pair are multiexponential and exhibit at least two lifetimes of 20 and 52 ns. In addition, a third lifetime of approximately 500 ps also appears to be present. These multiexponential charge-recombination kinetics reflect either different conformational states of D1/D2 reaction centers, with the different conformers exhibiting different radical pair lifetimes, or relaxations in the free energy of the radical pair state. Whichever model is invoked, the free energies of formation of the different radical pair states exhibit a linear temperature dependence from 100 to 220 K, indicating that they are dominated by entropy with negligible enthalpy contributions. These results are in agreement with previous determinations of the thermodynamics that govern primary charge separation in both D1/D2 reaction centers [Booth, P. J., Crystall, B., Giorgi, L. B., Barber, J., Klug, D. R., & Porter, G. (1990) *Biochim. Biophys. Acta 1016*, 141–152] and reaction centers of purple bacteria [Woodbury, N. W. T., & Parson, W. W. (1984) *Biochim. Biophys. Acta 767*, 345–361]. It is possible that these observations reflect structural changes that accompanying primary charge separation and assist in stabilization of the radical pair state thus optimizing the efficiency of primary electron transfer.

Photosystem 2 (PS2)[1] is responsible for the splitting of water to produce oxygen. The mechanism of this process remains obscure and is the subject of much research. A reaction center complex from PS2 known as the D1/D2 cytochrome *b*-559 complex has been successfully isolated (Nanba & Satoh, 1987; Barber et al., 1987). In the absence of modifications, the photosynthetic activity of the D1/D2 reaction center is limited to primary electron transfer, which results in the formation of the primary radical pair $P680^+Ph^-$. D1/D2 reaction centers contain the D1 and D2 polypeptides together with the apoproteins of cytochrome *b*-559 and the product of the *psb* I gene (Ikeuchi & Inoue, 1988; Webber et al., 1989). Although the D1/D2 reaction center is unable to evolve oxygen, the isolation of this complex has been of considerable importance to spectroscopic studies of PS2 as it has provided the first opportunity to study the kinetics of primary charge separation without the complication of subsequent quinone acceptors, antenna chlorophylls, and the oxygen evolving apparatus.

Isolated D1/D2 reaction centers have the reputation of being labile when exposed to light, which is due both to their susceptibility to damage by singlet oxygen (Crystall et al., 1989; McTavish et al., 1989; Durrant et al., 1990) and to an inbuilt light-activated autocatalytic protein cleavage (Shipton & Barber, 1991). This lability severely hampered initial time-resolved spectroscopic studies of D1/D2 reaction centers; however, they can now be stabilized sufficiently for such studies. This is achieved by removing all oxygen from the sample environment and solubilizing the reaction centers in a mild detergent such as dodecyl maltoside rather than Triton X-100 (Crystall et al., 1989; McTavish et al., 1989; Booth et al., 1990; Gounaris et al., 1990). Time-resolved fluorescence studies of such stabilized D1/D2 reaction centers indicate that they show high degrees of activity, with over 94% of the chlorophylls present being functionally coupled to electron transfer (Booth et al., 1990; Gounaris et al., 1990).

The kinetics of the primary radical pair in D1/D2 reaction centers have to date been studied in two ways. Transient absorption measurements have indicated that the primary radical pair decays with a lifetime of the order of 36 ns (Danielius et al., 1987; Takahashi et al., 1987). An alternative way to determine the lifetime of the radical pair is by monitoring "charge-recombination fluorescence" from P680*, which occurs as a result of charge-recombination of $P680^+Ph^-$ (Seibert et al., 1988; Mimuro et al., 1988; Crystall et al., 1989; Booth et al., 1990; Govindjee et al., 1990). Such measurements have also assigned a lifetime of 37 ns to the decay of the radical pair. These fluorescence measurements also indicated the presence of additional fluorescence components: a lifetime of 6.5 ns, which corresponds to chlorophyll that is energetically uncoupled from the process of primary charge separation (Booth et al., 1990), and some faster fluorescence components of a few nanoseconds or less whose origins have not been determined.

Primary electron transfer initiates photosynthetic electron transport and as such is central to photosynthetic activity. Primary electron transfer has attracted much theoretical and experimental interest (Jortner, 1980; Marcus & Sutin, 1985; Kirmaier & Holten, 1987; Bixon et al., 1989; Parson et al., 1990; Holzapfel et al., 1990), which has largely been centered on purple bacterial reaction centers due to the availability of a range of highly stabilized and well-characterized preparations. Despite considerable efforts, primary electron transfer is still not fully understood; indeed the very basis of the reaction

† This study was financially supported by the SERC, AFRC, and Royal Society. P.J.B. is a Unilever Junior Research Fellow at St. Hilda's College, Oxford, and D.R.K. is a Royal Society University Research Fellow.

* Author to whom correspondence should be addressed.
‡ Present address: Physical Chemistry Laboratory, Oxford University, South Parks Road, Oxford OX1 3QZ, U.K.
§ Present address: Department of Pharmaceutical Chemistry, University of Karachi, Karachi 75270, Pakistan.
∥ AFRC Photosynthesis Research Group.

[1] Abbreviations: CPC, counts in the peak channel; DBMIB, 2,5-dibromo-3-methyl-6-isopropyl-*p*-benzoquinone; FWHM, full width half-maximum; P, primary electron donor; P680, primary electron donor in PS2; Ph, pheophytin; PS2, photosystem 2; $Q_A$, secondary electron acceptor in PS2 and purple bacteria; SPC, single photon counting; TRES, time-resolved emission spectra.

0006-2960/91/0430-7573$02.50/0 

is still a matter for contention (Kirmaier & Holten, 1990; Marcus, 1990). A knowledge of the thermodynamics of primary electron transfer, and the reverse step of charge recombination, contributes to an understanding of the phenomena associated with this reaction. Time-resolved fluorescence measurements of highly active D1/D2 reaction center complexes have allowed the first determination of the free energy change associated with primary charge separation in D1/D2 reaction centers (Booth et al., 1990). The free energy gap was found to be −0.11 eV and appeared to be dominated by entropy over a wide temperature range. Fluorescence studies of *Rhodobacter sphaeroides* and *Rhodopseudomonas viridis* reaction centers have suggested essentially identical behavior for the corresponding free energy change in these bacterial reaction centers (Woodbury & Parson, 1984). D1/D2 reaction centers are thought to be similar to those of purple bacteria, particularly with regard to the cofactors involved in electron transport (Trebst, 1986; Barber, 1987; Michel & Deisenhofer, 1988), and the similarity of the thermodynamics of primary charge separation further strengthens the resemblance between the two types of reaction center.

In this paper we present more detailed time-resolved absorption and fluorescence measurements of the primary radical pair kinetics in D1/D2 reaction centers. These data indicate that the results obtained from earlier studies do not fully represent the radical pair dynamics. In addition the origins of the fastest fluorescence components are assigned to processes in the reaction center. These results provide further insight into the nature of the primary radical pair in PS2 and indicate that the simple reaction scheme proposed earlier for D1/D2 reaction centers (Booth et al., 1990) is incomplete. The thermodynamics that govern primary charge separation in D1/D2 reaction centers are reexamined in view of these results.

## Materials and Methods

*Sample Preparation.* The D1/D2 reaction center was isolated from pea thylakoid membranes. The complex was prepared by Triton X-100 solubilization of PS2-enriched membranes as described by Chapman et al. (1988) with the second chromatographic separation carried out in a buffer containing 2 mM dodecyl maltoside as described by Chapman et al. (1991a). The D1/D2 complex bound chlorophyll *a*, pheophytin, and $\beta$ carotene in the ratio 6:2:2 (Gounaris et al. 1990). The preparation was stored at 77 K.

D1/D2 reaction center samples were resuspended in two types of buffer, either buffer A, 50 mM Tris-HCl at pH 8 or buffer B, 20 mM Bis-Tris, 20 mM NaCl, 10 mM $MgCl_2$, and 1.5% taurine at pH 6.5. (pH values are quoted for room temperature.) Dodecyl maltoside was added to the buffers, details of the concentrations are given in the text. Reaction center samples were resuspended to give final chlorophyll concentrations of 10–20 $\mu$g mL$^{-1}$ for fluorescence measurements and 20 $\mu$g mL$^{-1}$ for transient absorption measurements. This difference in chlorophyll concentration had no apparent effect on the kinetics observed, and the higher concentration was used in some cases to improve the signal to noise ratio of the measurements.

It is important to minimize the degree of aggregation in D1/D2 reaction center samples to guarantee consistent kinetic behavior. Extensive aggregation is observed as a shortening of the fluorescence lifetimes and/or red-shifts of the reaction center, long-wavelength absorption and fluorescence bands by 1–2 nm. Such aggregation was caused by reducing the concentration of dodecyl maltoside to a level close to the critical micelle concentration of 0.2 mM. At concentrations of 0.6 mM or above, no aggregation was apparent; however, overly high detergent concentrations reduced the stability of the D1/D2 reaction centers.

It is essential to ensure consistently high electron transfer activity of D1/D2 reaction center samples, particularly for the fluorescence measurements (Booth et al., 1990). All "active" D1/D2 reaction center samples showed long-wavelength absorption and fluorescence band maxima of 676.0 ± 0.5 nm and 683 ± 1 nm before and after all measurements. Once samples were thawed and resuspended in either buffer A or B, they were used immediately and were not stored overnight. All experiments on active D1/D2 reaction center samples were performed under anaerobic conditions, which were achieved as described by Booth et al. (1990). Samples solubilized in buffer B containing 1 mM dodecyl maltoside were stable to laser excitation of 20–30 mW average power at 620 nm for at least 1 h at 293 K.

Braun et al. (1990) have reported a fluorescence maximum of 685 nm for active D1/D2 reaction centers. In contrast, we have only observed maxima red-shifted from 683 nm, from aggregated D1/D2 reaction center samples and at low temperatures. Similarly, Tetenkin et al. (1989) have also reported a red-shifted fluorescence maximum, of approximately 686 nm, from reaction centers in the absence of Triton X-100, which are presumably aggregated. These differences in the fluorescence maxima of active D1/D2 reaction center samples (of 683 nm reported by us and 685 nm reported by Braun et al.) could also be connected with variations in the stoichiometry of the reaction centers studied. Braun et al. studied reaction centers that contained four chlorophylls per two pheophytins whereas the reaction centers studied here apparently contain six chlorophylls per two pheophytins. It is possible that the two additional chlorophylls may cause a relative blue-shift in the fluorescence band. Reliable stoichiometries are, however, difficult to obtain.

Variable temperature measurements were made with an Oxford Instruments DN 1704 liquid nitrogen cryostat. Samples were suspended in buffer B containing 1 mM dodecyl maltoside and 50% glycerol for these measurements (Booth et al., 1990).

*Steady-State Spectroscopy.* Steady-state absorption measurements were made with a Perkin-Elmer 554 spectrometer with a bandwidth of 1 nm. Errors quoted for absorption wavelengths are estimates of accuracy limitation.

Steady-state fluorescence spectra were made with a Perkin-Elmer MPF-4 fluorimeter with excitation and emission bandwidths of 2 nm and excitation at 405 nm. Imprecisions quoted for fluorescence wavelengths are due to the detection bandwidth used. Steady-state fluorescence yields were obtained for active D1/D2 reaction center samples by integrating over the fluorescence band from 640 to 710 nm. Steady-state fluorescence yields for inactive samples and for monomeric chlorophyll *a* in ether were obtained by integrating over an equivalent range.

*Time-Resolved Fluorescence Measurements.* Fluorescence lifetimes were measured by the technique of time-correlated single photon counting, SPC (O'Connor & Phillips, 1984). The apparatus was essentially as described by Booth et al. (1990). The instrument response function had a FWHM of approximately 100 ps, giving time resolution after deconvolution of the order of 20–30 ps. A 650-nm cut-off filter was used in fluorescence measurements to eliminate any laser scatter. A 615-nm (40-nm FWHM) band-pass filter was used during measurements of the instrument response function.

Samples were illuminated at 615 or 620 nm with an average power of 20–30 mW at 3.7 MHz. A volume of 0.1 cm$^3$ of

Table I: Time Scales Used for SPC Measurements

| timescale | time per collection channel (ns) | full scale (ns) |
|---|---|---|
| 1 | 0.560 | 280 |
| 2 | 0.180 | 92 |
| 3 | 0.006 | 3 |

sample was illuminated by the laser, and less than 1 in $10^4$ of the reaction centers present in this volume were excited by each laser pulse (Booth et al., 1990). The steady-state population of triplet P680 was less than 2% of the reaction centers present in the illuminated volume. Samples were stirred in SPC experiments performed at 277 K or above.

SPC measurements were taken on the three time scales shown in Table I, unless otherwise stated.

One of the problems associated with measurements on D1/D2 reaction center samples, which have low fluorescence yields, over such a short time scale as time scale 3 is the relatively long time required to accumulate high CPC. For example, accumulation of 20 000 CPC on time scale 3 takes approximately 1 h, compared with 5 min on time scale 2. In order to reduce the effect of laser instabilities and to ensure that the samples were intact throughout data collection, fluorescence decays were only collected to 10 000 CPC on time scale 3. The results from several decays were then analyzed globally to improve the confidence level of the results. For these measurements, D1/D2 reaction centers were solubilized in buffer B containing 1 mM dodecyl maltoside, under anaerobic conditions. Although a lower detergent concentration improves the stability of the samples to laser excitation, it can result in some aggregation of the samples, which typically results in an increase in the amount of fast fluorescence components.

Time-resolved emission spectra (TRES) were collected by scanning the detection wavelength from 650 to 705 nm.

*Transient Absorption Measurements.* Measurements were made with the flash photolysis apparatus described previously (Durrant et al., 1990), with the following modifications. The probe beam was provided by a 35 mW laser diode (Mitsibushi ML5415N), with the wavelength centered at 820 nm, and detected with a silicon photodiode (EG&G FN100) with gated bias connected to a home-built amplifier incorporating a 4.7-$\mu$s high-pass filter. The time resolution of the apparatus is limited by the amplifier, which has a 10–90% rise time of 4 ns. An 820-nm (10-nm bandwidth) interference filter was placed in front of the detector to improve fluorescence rejection. There is no fluorescence contribution to the data, partly due to the small solid angle of detection.

Samples were excited at 337 nm with 800-ps pulses at a repetition rate of 3 Hz and a pulse energy of 0.45 mJ. The optical path length was 1 cm. The data presented here are the average of 64 flashes.

*Analysis.* Lifetimes were calculated by iterative reconvolution based on the Marquardt fitting algorithm (Marquardt, 1963), assuming multiexponential decay kinetics. The quality of fits was judged by using a reduced $\chi^2$ criterion and plots of the weighted residuals. Data sets were analyzed individually and up to 12 data sets could be analyzed globally. In both cases the data were fit to up to four exponentials with the option of fixing the value of one or more lifetimes. Global analysis (Knutson et al., 1983) reduces the effects of exponential correlation and improves the accuracy of parameters extracted from data.

In order to check the validity of our kinetic assignments, fluorescence data were collected over several time scales (from 3 to 280 ns full scale) to ensure adequate data density over the complete range of lifetimes studied. Over-parameterization was tested for using stimulated data studies (see Appendix A). Simulated decays were generated containing a number of exponentials (1–10) to which constant background and Poisson-type noise were added.

Fluorescence decays from active D1/D2 reaction centers collected on time scale 1 were well represented by the sum of four exponentials. The shortest resolved component had a lifetime of approximately 200 ps and an amplitude that varied from positive to negative values between data sets. On time scale 1 the instrument response function (approximately 100 ps) was less than the channel time (560 ps), therefore this short component largely represents the inability to adequately fit the instrument response. In fact the data could also be adequately fit by three exponentials and an additional variable component to take account of instantaneous scatter or very short lived emission. (Appropriate use of filters ensures that there is in fact no laser scatter present in these data.) In such a three-exponential fit, the three lifetimes were the same as the three longer lifetimes resulting from the four-exponential fit. In general, fitting to four exponentials gave a better fit than fitting to three plus "scatter", so all results from time scale 1 are from four-exponential fits to the data. The shortest component actually reflects the difficulty in obtaining good fits over the instrument response function rather than a genuine physical component; values for this component are not quoted. On this long time scale, it is not possible to accurately determine lifetimes of $<1$ ns.

For low-temperature measurements, several fluorescence decays were collected on time scale 1 at a particular temperature and globally analyzed. In these fits a lifetime was fixed at 5 ns to represent uncoupled chlorophyll; the lifetime of which is independent of temperature (Booth et al., 1990). The fixed value chosen was 5 ns rather than 6.5 ns [as previously used by Booth et al. (1990)] in agreement with results from a free running fit to data on time scale 1, at 293 K (see Results and Table III).

Details of the analysis of fluorescence decays on time scale 2 have already been reported by Booth et al. (1990).

Fluorescence decays from active D1/D2 reaction centers on time scale 3 were fit to three exponentials. Fitting the data to four exponentials did not significantly improve the fits. On time scale 3 the "37-ns" and "6.5-ns" components cannot be differentiated and appear as one lifetime. This presented problems in analysis of the decays. Over 3 ns, the 6.5-ns component will decay significantly and contribute to the overall fluorescence decay of the sample; however, the 37-ns component is essentially unchanged over 3 ns and appears as a background to the decay; however, it was not possible to fix the background during a global analysis. As a result, fluorescence decays on time scale 3, when analyzed globally, were best represented by the sum of three exponentials with the 37-ns and 6.5-ns components appearing as one lifetime.

All yields of fluorescence components are relative and are quoted as the integral of the appropriate component of the fluorescence decay. Errors in yields and lifetimes are quoted as one standard deviation.

Transient absorption decays were fit to three and four exponentials. In these fits a lifetime was fixed (at 4.7 $\mu$s) to represent the filtered decay of triplet P680 in D1/D2 reaction centers, while all other parameters were free running. The parameters associated with the fixed-lifetime component are not quoted. Triplet P680 decays with a lifetime of approximately 1 ms in the absence of oxygen (Mathis et al., 1989; Durrant et al., 1990). However, the use of a 4.7-$\mu$s filter in

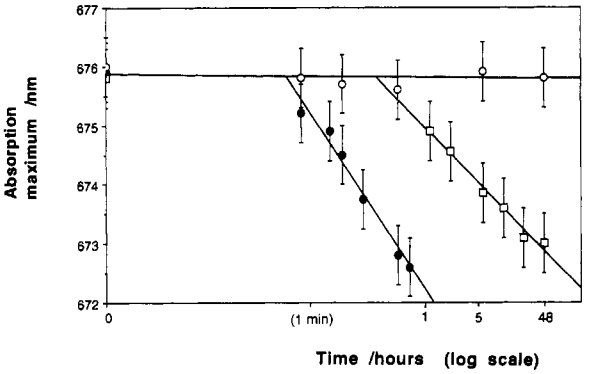


FIGURE 1: Stability of D1/D2 reaction centers solubilized in dodecyl maltoside under aerobic conditions. Dependence of long-wavelength absorption band maximum on time when samples were exposed to continuous white light of 500 $\mu$E $m^{-2}$ $s^{-1}$ at 277 K (●) or to a temperature of 293 K in the dark (□); (○) denotes dark controls at 277 K. Samples were suspended in buffer A containing 2 mM dodecyl maltoside.

Table II: Results of Time-Resolved Fluorescence Measurements on Active and Damaged D1/D2 Reaction Center Samples[a]

| decay | $\lambda_{abs} \pm 0.5$ (nm)[b] | $\tau_1 \pm 2.0$ (ns)[c] | $F_1 \pm 4$ (%)[d] | $F_2 \pm 4$ (%)[e] |
|---|---|---|---|---|
| 1 | 675.9 (active) | 36.5 | 44 | 40 |
| 2 | 674.8 | 38.6 | 24 | 44 |
| 3 | 674.1 | 38.1 | 15 | 59 |
| 4 | 673.5 | 18.6 | 3 | 62 |
| 5 | 672.9[f] | $10^4$ | negative amplitude | |

[a] Samples were suspended in buffer A containing 2 mM dodecyl maltoside, under anaerobic conditions, and degradation was induced by 20 mW laser illumination at 615 nm. [b] Long-wavelength absorption maximum. [c] Charge-recombination fluorescence lifetime. [d] Relative yield of charge-recombination fluorescence. [e] Relative yield of uncoupled chlorophyll fluorescence. [f] Fluorescence decays with long-wavelength absorption maxima less than 673 nm were best represented by the sum of two exponentials, with the majority of the fluorescence from a 6-ns component and the remainder from a 1-ns component (Booth et al., 1990).

conjunction with the detection photodiode (see above) means that the triplet lifetime is seen as 4.7 $\mu$s. Deconvolution of the transient absorption data by using the instrument response function from this apparatus results in an effective time resultion of 1 ns with accuracy of ±1 ns.

*Electron Transfer Activity of D1/D2 Reaction Centers.* The intact D1/D2 reaction center is characterized by a long-wavelength absorption maximum at approximately 676 nm (Chapman et al., 1989; Booth et al., 1990; Braun et al., 1990), while degradation of the reaction center is observed as blue-shifts in this peak (see Figure 1).

Fluorescence decays were collected on time scale 2 from D1/D2 samples having different long-wavelength absorption maxima. Table II shows the results of individually analyzing these fluorescence decays to four exponentials with a lifetime fixed at 6.5 ns to represent uncoupled chlorophyll. The decays were also analyzed globally. In a free-running three-exponential global analysis, the lifetimes were resolved as 36, 6, and 1 ns. (A fourth lifetime was not required to accurately model the two longest components in this global analysis on time scale 2.) Figure 2 shows the relationship between the relative fluorescence yield of these components and the long-wavelength absorption maxima.

An analysis of simulated fluorescence decays indicates that the results shown in Table II are in fact consistent with the lifetime of charge-recombination fluorescence remaining constant as the reaction centers are damaged (see Appendix A). The apparent reduction in the charge-recombination

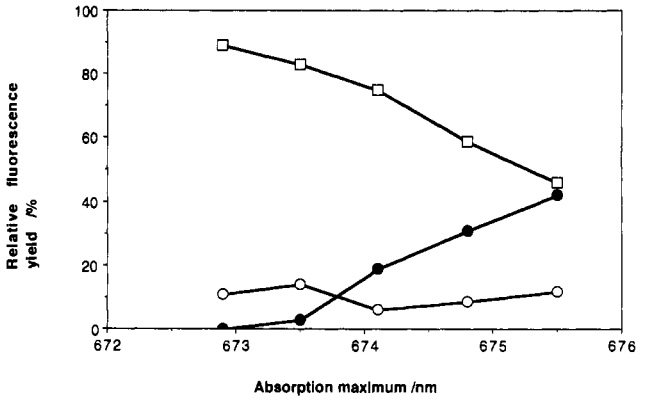


FIGURE 2: Dependence of the relative fluorescence yields of time-resolved fluorescence components on position of long-wavelength absorption maximum of D1/D2 reaction centers. (●) charge-recombination fluorescence; (□) uncoupled chlorophyll fluorescence; (○) fast fluorescence components.

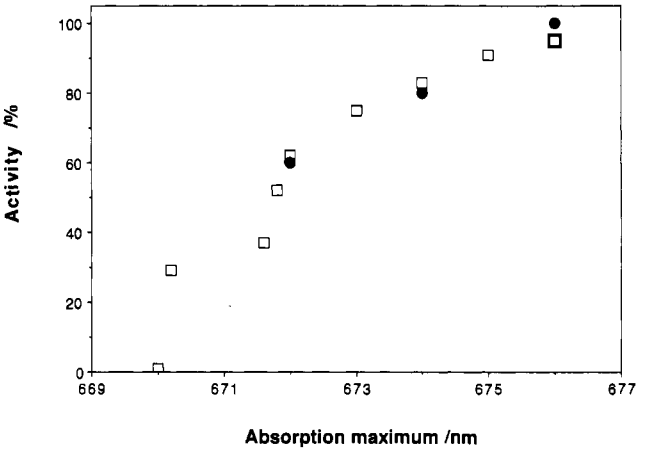


FIGURE 3: Relationship between activity of D1/D2 reaction center samples and their long-wavelength absorption band maximum. (□) Percent of chlorophylls in D1/D2 reaction center samples that are functionally coupled to charge separation; (●) percent of active reaction centers as determined by Braun et al. (1990).

fluorescence lifetime shown in Table II reflects correlation of the 37-ns and 6.5-ns components as their relative yields alter. Figure 2 shows that as the absorption maximum shifts to the blue there is an increase in the relative fluorescence yield of uncoupled chlorophyll and decrease in that of charge-recombination fluorescence. Concomitant with the increase in the uncoupled chlorophyll fluorescence yield is an increase in the total steady-state fluorescence yield of D1/D2 reaction centers [see Figure 2 of Booth et al. (1990)].

The proportion of damaged D1/D2 reaction centers can be found from the ratio of the relative yield of the uncoupled chlorophyll fluorescence to that of monomeric chlorophyll *a* in ether (chlorophyll in both these environments has the same fluorescence lifetime and therefore quantum yield) (Booth et al., 1990). The dependence of the relative fluorescence yield of the 6.5-ns component on long-wavelength maximum (see Figure 2) together with that of the steady-state fluorescence yield of D1/D2 reaction center samples [see Figure 2 of Booth et al. (1990)] allows the proportion of damaged D1/D2 reaction centers to be determined as a function of long-wavelength absorption maximum. This in turn allows the relationship between the degree of electron transfer activity of D1/D2 reaction centers (as determined by the percentage of chlorophylls that are coupled to primary electron transfer) and the long-wavelength absorption maximum to to be found (see Figure 3). Also shown in Figure 3 is the percentage of active

Table III: Decay Kinetics of the Primary Radical Pair in D1/D2 Reaction Centers As Determined by Time-Resolved Fluorescence and Absorption Measurements

| | fluorescence data | | |
|---|---|---|---|
| | time scale 2, 92-ns full scale[a] | time scale 1, 280-ns full scale | absorption data 512-ns full scale |
| component | $\tau$ (ns)[b] | $\tau$ (ns)[b] | $\tau$ (ns)[c] |
| RP-1 | $36.5_{(44)}$ | $52.1_{(25\pm2)}$ | $56 \pm 3_{(42\pm7)}$ |
| RP-2 | | $20.1_{(19\pm1)}$ | $19 \pm 7_{(18\pm11)}$ |
| UC-1 | $6.5_{(40)}$ | $5.3_{(56\pm2)}$ | |
| SH-1 | $1.5_{(11)}$ | | $2 \pm 2_{(31\pm9)}$ |
| SH-2 | $0.1_{(5)}$ | | |

[a] Crystall et al. (1989). [b] Relative fluorescence yields, in percent, are shown in parentheses as subscripts to fluorescence lifetimes. [c] Relative amplitudes, in percent, are shown in parentheses as subscripts to lifetimes.

reaction centers as determined by Braun et al. (1990) as a function of absorption peak. Braun et al. determined activities by steady-state spectral characterization of D1/D2 reaction centers (solubilized in Triton X-100).

## Results

### *Time-Resolved Fluorescence Measurements on Active D1/D2 Reaction Center Samples*

*(A) Details of Charge-Recombination Fluorescence.* Figure 4 shows a typical fluorescence decay collected from an active D1/D2 reaction center sample on time scale 1. The fluorescence decay shown in Figure 4 is best represented by the sum of four exponentials; the $\chi^2$ for a four-exponential fit is 1.16, while that for a three-exponential fit is 6.94.

To determine the values of the fluorescence lifetimes on time scale 1, five fluorescence decays (each to 60 000 CPC) were analyzed globally to four exponentials with all parameters free running. The results are given in Table III (column three). (Parameters for the shortest component are not shown; see Analysis.) Measurements on a time scale longer than time scale 1, with a 320 ns full scale, gave results similar to those of time scale 1.

*Interpretation.* In Table III the results of these fluorescence decays on time scale 1 are compared to previous results on time scale 2 with 20 000 CPC by Crystall et al. (1989) (see column two). Comparison of these data shows that the lifetime that was previously resolved as 37 ns and assigned to charge recombination of $P680^+Ph^-$ is actually an average of two lifetimes of 20 and 52 ns (the latter two lifetimes will be referred to as RP-2 and RP-1, respectively). Analysis of simulated fluorescence decays (see Appendix A) illustrates that the curve-fitting algorithm is in fact unable to distinguish lifetimes of 20 and 52 ns on time scale 2.

In order to rule out variable sample behavior, fluorescence decays were collected from the same sample on both time scales 1 and 2, at 293 K. The results were consistent with the data shown in Table III; a lifetime of 37 ns was resolved on time scale 2 and lifetimes of 20 and 52 ns on time scale 1.

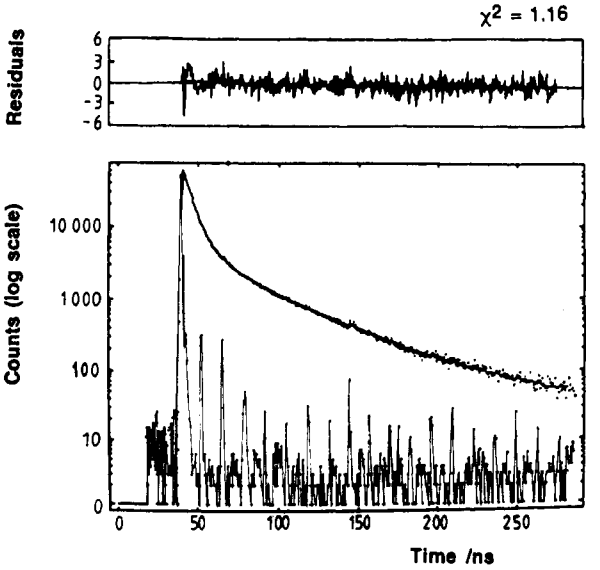


FIGURE 4: Typical fluorescence decay from D1/D2 reaction centers on time scale 1, at 293 K, measured at 683 nm with a 6-nm bandwidth, to 60 000 CPC. Also shown are the $\chi^2$ value and residuals for a four-exponential fit to the data. The sample was exposed to 30 mW average power at 615 nm, and accumulation of 60 000 CPC took approximately 5 min. The instrument response function is shown below the fluorescence decay.

SPC measurements of D1/D2 reaction centers on time scale 1 also resolve a lifetime of 5 ns in addition to the two longer lifetimes of 20 and 52 ns. This corresponds to chlorophyll that is uncoupled from the process of charge separation and was also observed in previous fluorescence studies on time scale 2 (Crystall et al., 1989; Booth et al., 1990; Gounaris et al., 1990). In these earlier studies, this fluorescence lifetime was resolved as 6.5 ns; however, this slight difference in lifetime probably reflects differing effects of exponential correlation in the data from the two time scales. This uncoupled chlorophyll fluorescence will be referred to as UC-1. The relative yields of the fluorescence components obtained from decays measured on time scales 1 and 2 are entirely consistent (see Table III). In both cases approximately half of the fluorescence is due to uncoupled chlorophyll while the remainder is dominated by the longer charge-recombination components.

*(B) Temperature Dependence of the Fluorescence Components.* The temperature dependences of components RP-1 and RP-2 were determined by measuring fluorescence decays on time scale 1 at temperatures between 100 and 293 K. The results of analysis of these decays are shown in Table IV (columns two and three).

A slight shift in the fluorescence maximum of D1/D2 reaction center samples was observed as the temperature was reduced: from 683 nm at 293 K to 686 nm at 100 K. Such

Table IV: Equilibrium Constants and Free Energies of Formation for Radical Pair States RP-1 and RP-2 as a Function of Temperature

| | $\tau \pm 2.0$ (ns)[a] | | $\phi \pm 0.2$ (%)[b] | | $K \pm 13$[c] | | $-\Delta G \pm 0.003$ (eV)[d] | |
|---|---|---|---|---|---|---|---|---|
| $T$/K | RP-2 | RP-1 | RP-2 | RP-1 | RP-2 | RP-1 | RP-2 | RP-1 |
| 293 | $20.1_{(19)}$ | $52.1_{(25)}$ | 0.7 | 0.9 | 49 | 194 | 0.100 | 0.135 |
| 260 | $25.5_{(6)}$ | $65.8_{(3)}$ | 0.2 | 0.2 | 224 | 1154 | 0.121 | 0.158 |
| 230 | $16.4_{(15)}$ | $57.0_{(26)}$ | 0.5 | 0.8 | 58 | 250 | 0.081 | 0.110 |
| 200 | $21.1_{(21)}$ | $72.5_{(16)}$ | 1.2 | 0.8 | 31 | 318 | 0.059 | 0.099 |
| 130 | $23.1_{(18)}$ | $76.7_{(16)}$ | 0.6 | 0.6 | 68 | 449 | 0.047 | 0.068 |
| 100 | $20.3_{(14)}$ | $85.3_{(13)}$ | 0.6 | 0.5 | 59 | 599 | 0.035 | 0.055 |

[a] Relative fluorescence yields, in percent, are shown as subscripts to fluorescence lifetimes. [b] Fluorescence quantum yield. [c] Equilibrium constant for conformational substate model. [d] Free energy of formation of radical pair state for conformational substate model.

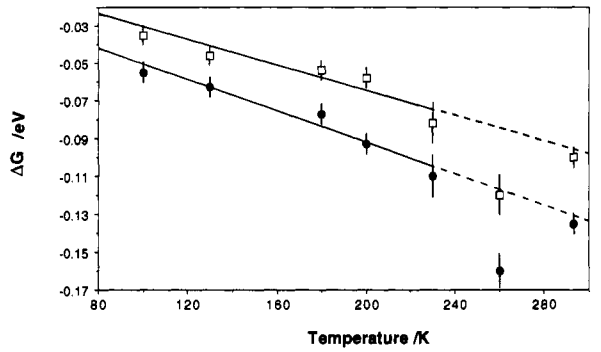


FIGURE 5: $\Delta G$(P680$^+$Ph$^-$–P680*) in D1/D2 reaction centers as a function of temperature; and $\Delta G$(P680$^+$Ph$^-$–P680*) for radical pair states (●) RP-1 and (□) RP-2, respectively ($\Delta G_{RP\text{-}1}$ and $\Delta G_{RP\text{-}2}$), calculated for a conformational substate model. The corresponding $\Delta G$ curves for a sequential relaxation model were essentially identical with these curves but were vertically displaced by <0.01 eV. For the details of the models see Discussion.

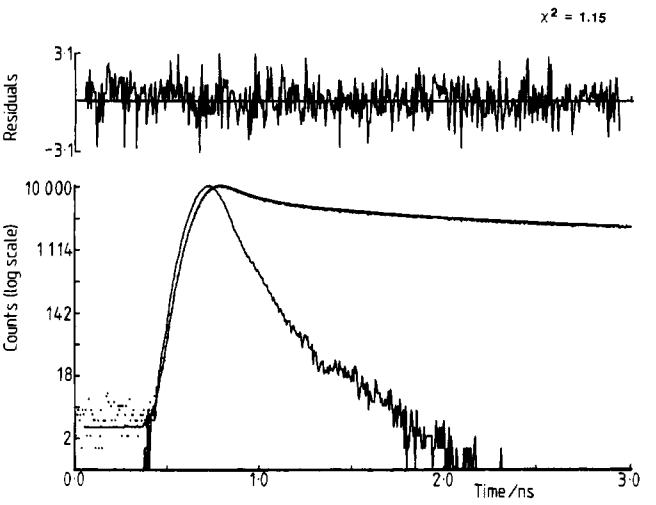


FIGURE 6: Typical fluorescence decay from D1/D2 reaction centers on time scale 3, at 277 K, measured at 683 nm with a 6-nm bandwidth, to 10000 CPC. Also shown are the $\chi^2$ value and residuals for a three-exponential fit to the data. The instrument response function is shown below the fluorescence decay.

a shift was not observed in previous measurements (Booth et al., 1990) due to the wider collection bandwidth of 6 nm used in these earlier experiments. A 3-nm collection bandwidth was used in the measurements reported here.

The variation of steady-steady fluorescence yield of D1/D2 reaction center samples with temperature has already been reported [see Figure 5 of Booth et al. (1990)].

(*C*) *The Free Energy of Primary Charge Separation, $\Delta G$(P680$^+$Ph$^-$–P680*).* It is possible to calculate the absolute quantum yields of fluorescence components RP-1 and RP-2 by comparison with monomeric chlorophyll *a* in ether (Booth et al., 1990). The results are given in Table IV (columns four and five). Also shown in Table IV are the equilibrium constants at 293 K, $K_{RP\text{-}1}$ and $K_{RP\text{-}2}$, for the equilibria (P680* ⇌ P680$^+$Ph$^-$) established on time scales of 52 and 20 ns, respectively, and the free energy differences $\Delta G$(P680$^+$Ph$^-$–P680*), $\Delta G_{RP\text{-}1}$, and $\Delta G_{RP\text{-}2}$, which correspond to $K_{RP\text{-}1}$ and $K_{RP\text{-}2}$. Figure 5 shows the variation of $\Delta G_{RP\text{-}1}$ and $\Delta G_{RP\text{-}2}$ with temperature. Details of the free energy calculations are given in Appendix B. Table IV shows results of these calculations for the "conformational substate" model (see Discussion). The "sequential relaxation" model (see Discussion) gives similar results: $K_{RP\text{-}2}$ = 98, $K_{RP\text{-}1}$ = 291, $\Delta G_{RP\text{-}2}$ = −0.116 eV, and $\Delta G_{RP\text{-}1}$ = −0.143 eV.

*Interpretation.* A discussion of the accuracy in measurements of $\Delta G$(P680$^+$Ph$^-$–P680*) has already been given (Booth et al., 1990). The dominant limitation in the accuracy is the value used for the natural lifetime of P680*, which introduces, at most, a 10% error in the magnitude of $\Delta G$ (Booth et al., 1990). Some uncertainty in the precision of $\Delta G$ also comes from uncertainties in the charge-recombination fuorescence quantum yield $\phi_1$ and lifetime $\tau_1$, giving an uncertainty of ±0.003 eV (Booth et al., 1990). Both these contributions to the uncertainty in the value of $\Delta G$ affect the absolute values for the $\Delta G$'s quoted in Table IV, but not the difference in the values. Therefore the difference between $\Delta G_{RP\text{-}1}$ and $\Delta G_{RP\text{-}2}$ is significant.

The magnitude of both $\Delta G_{RP\text{-}1}$ and $\Delta G_{RP\text{-}2}$ increases linearly with temperature from 100 to 230 K (see Figure 5). These temperature dependences are the same as that previously found for the free energy of charge separation determined from fluorescence measurements on time scale 2 (Booth et al., 1990) and also to the free energy of primary charge separation for *Rb. sphaeroides* reaction centers as determined by Woodbury and Parson (1984) [see Figure 8 of Booth et al. (1990)].

(*D*) *Fastest Fluorescence Components.* Figure 6 shows a typical fluorescence decay from D1/D2 reaction centers on time scale 3. The decay is best fit by three exponentials. In a global analysis of five such fluorescence decays, the two shortest components are resolved as approximately 500 and 50 ps when the longest lifetime is fixed (arbitrarily) at 6.5 ns. (The 500-ps and 50-ps components will be referred to as SH-1 and SH-2, respectively.) On time scale 3 components RP-1, RP-2, and UC-1 cannot be differentiated and appear as one lifetime (see Analysis). The greater the value to which this long lifetime is fixed, the longer the lifetimes resolved for SH-1 and SH-2 (and the lower their fluorescence yields); when the long component is fixed at 20 ns, the lifetimes of SH-1 and SH-2 are resolved as 676 and 53 ps, respectively.

(*E*) *Time-Resolved Emission Spectra (TRES).* Time windows were selected that corresponded to the maximum contribution of the individual fluorescence components. Figure 7A compares TRES spectra for time windows of 0–10 ns and 120–240 ns. The latter window essentially represents only RP-1 as the other components have all decayed by this time. The ratio of the relative contributions of RP-1 to RP-2 is 100 to 1, in the 120–240 ns window. The 0–10 ns window is dominated by UC-1, with the ratio of contributions of UC-1 to SH-1 and SH-2 being 3 to 1, and the relative contribution of UC-1 to RP-2 being 5 to 1.

It is difficult to select time windows that are strongly dominated by SH-1 and SH-2. However, TRES obtained with greater contributions of these faster fluorescence components indicated that the short time emission was broadened compared to both spectra RP-1 and UC-1, with a maximum around 680 nm. The TRES narrowed as the contribution from the shortest component (SH-2) was increased.

To further investigate the emission spectra of the fluorescence components, fluorescence decays were collected at different wavelengths from 650 to 700 nm and globally analyzed. (Such an analysis assumes that the lifetimes of the various fluorescence components are independent of wavelength.) Figure 7B shows the wavelength dependence of the relative yields of RP-1 and UC-1. RP-2 had a spectrum essentially identical with that of RP-1.

Figure 7C shows the wavelength dependence of the relative yields of SH-1 and SH-2. (Note that the errors in yields and wavelength are greater than in Figure 7B.)

*Interpretation.* It is clear that the TRES of RP-1 is more asymmetric and red-shifted than that of UC-1. The emission

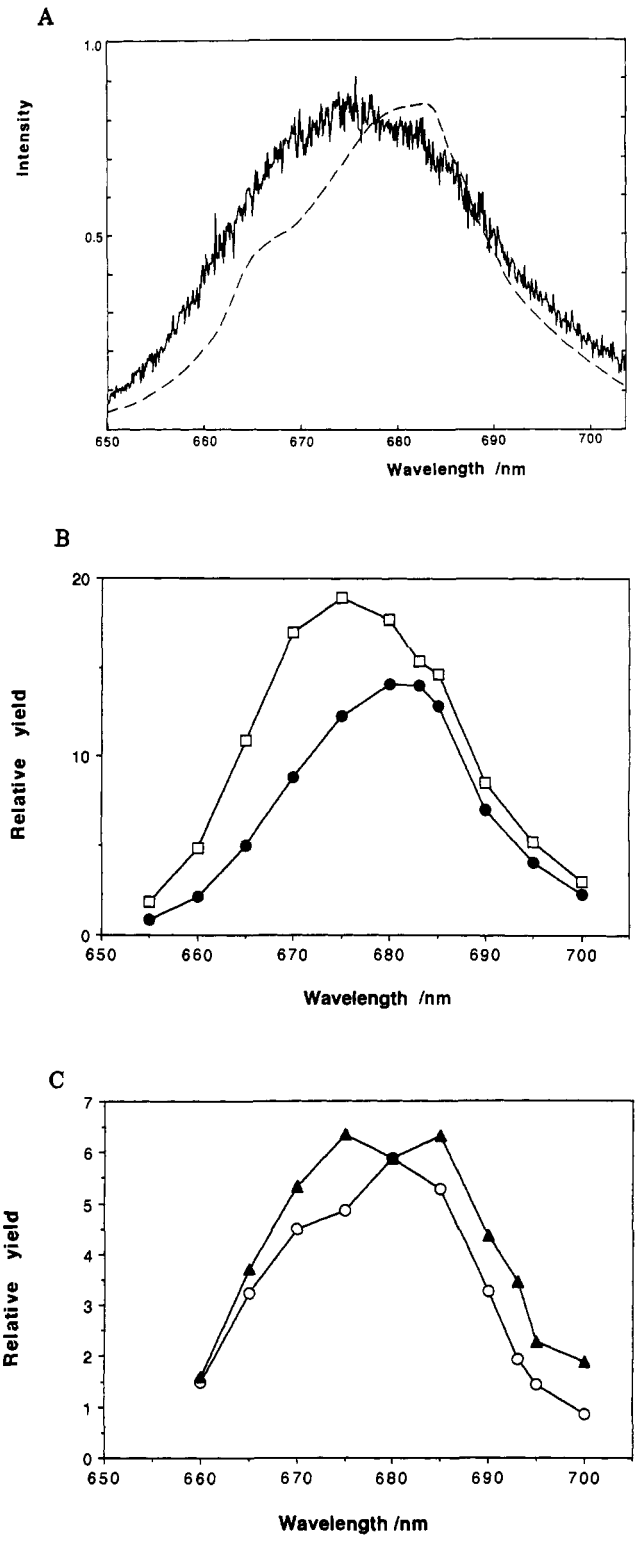


FIGURE 7: (A) TRES spectra from D1/D2 reaction centers obtained with a detection bandwidth of 3 nm; (–) spectrum of UC-1 and (– – –) spectrum of RP-1. Intensity is in arbitrary units. (B) Wavelength dependence of relative yields of fluorescence components RP-1 (●) and UC-1 (□), which was determined by global analysis of fluorescence decays on a time scale of 485 ps per channel, giving 250–ns full scale. Each decay was measured with a 3-nm bandwidth to 40 000 CPC. The error bars for the yields fall within the symbols. The relative fluorescence yield is in arbitrary units. (C) Wavelength dependence of relative yields of fast fluorescence components SH-1 (▲) and SH-2 (○). Determined by global analysis of fluorescence decays on a time scale of 12 ps per channel, giving 6-ns full scale. Individual decays were measured with a 6-nm bandwidth to a maximum of 4000 CPC. Relative yields shown are an average of four global wavelength sets and are in arbitrary units. Errors in the yields are ±0.7.

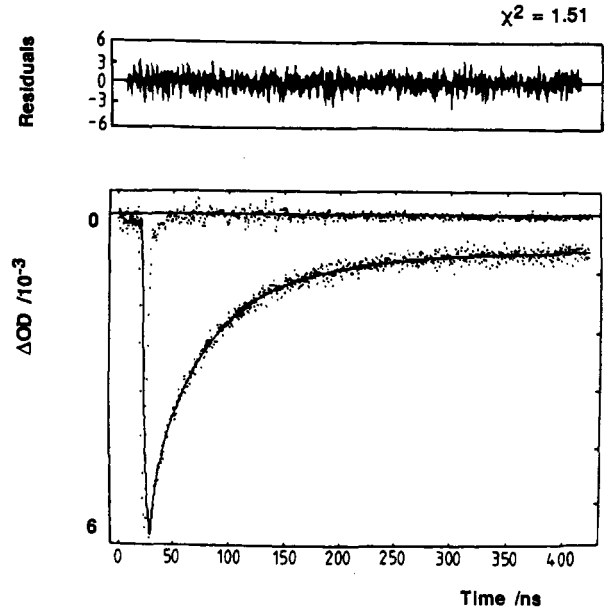


FIGURE 8: Typical absorption decay from D1/D2 reaction centers, at 293 K. Measured at 820 nm on a time scale of 500 ps per channel, giving 512-ns full scale. Also shown are the $\chi^2$ value and residuals for a three-exponential fit to the data. The instrument response function is shown above the decay. Note that ΔOD is shown inverted and on a linear scale.

maximum of the former is centered at approximately 683 nm while that of the latter peaks at about 676 nm. Spectrum UC-1 is also broader, having a FWHM of the order of 32 nm as compared to that of RP-1 of approximately 25 nm. Spectrum RP-1 also has a slight shoulder at around 670 nm that contributes to its bandwidth. The spectra shown in Figure 7B have the same features as these TRES. The apparent difference in relative yields of RP-1 and UC-1 in Figure 7A,B reflects slightly different activities of the D1/D2 reaction center preparations studied.

Both spectra SH-1 and SH-2 peak at approximately 680 nm, which is slightly to the red of that of UC-1 (see Figure 7A,B). In addition, spectrum SH-1 has a very broad bandwidth.

Similar results and TRES spectra from D1/D2 reaction centers have been reported by Mimuro et al. (1988). Mimuro et al. only resolved a single long charge-recombination lifetime of 35 ns that had a maximum emission wavelength at 682 nm. A 25-ps fluorescence component was also found to have an emission maximum at 682 nm. In addition there was also some fluorescence resulting from chlorophyll *a* in the reaction center samples that had emission maxima at 676 and 670 nm.

### *Transient Absorption Measurements of $P680^+Ph^-$*

Figure 8 shows typical decay kinetics at 820 nm of D1/D2 reaction centers. The decay is adequately fit by three exponentials and fitting the decay to four exponentials only slightly improves the $\chi^2$ value and residuals. In these fits one lifetime represents the decay of triplet P680 in the reaction center samples, and therefore at least two exponentials are required to model the radical pair decay kinetics. In a three-exponential fit to the data, these two lifetimes are resolved as 54 and 8 ns. When the data are fit to four exponentials, the lifetimes are resolved as 56, 19, and 2 ns (see Table III, column four). The results shown in Table III are an average of fitting five data sets to four exponentials; the parameters for the triplet component are not shown.

The radical pair quantum yield can be calculated from the data of Figure 8 as 1.1 ± 0.2, assuming a $P680^+Ph^-$ extinction

coefficient of 12 400 (Mathis & Setif, 1981; Fujita et al., 1978). The triplet yield quantum yield is calculated from these data as 0.3 ± 0.1, in agreement with previous measurements (Takahashi et al., 1987; Durrant et al., 1990).

## Discussion

### *Radical Pair Kinetics*

(*A*) *Time-Resolved Fluorescence Measurements.* Previous time-resolved fluorescence measurements on active D1/D2 reaction centers assigned a lifetime of 37 ns to charge recombination of the primary radical pair (Crystall et al., 1989; Booth et al., 1990). However, when fluorescence measurements are taken on a longer time scale (time scale 1), it becomes apparent that this 37-ns lifetime is actually an average of two lifetimes of approximately 20 and 52 ns (see Table III).

The measurements on a much shorter time scale (time scale 3) allow the fastest fluorescence components, SH-1 and SH-2, to be examined. These measurements show that there are two fast components with lifetimes of the order of 50 and 500 ps. The effect of the quinone DBMIB on components SH-1 and SH-2 was investigated (Booth, 1990). DBMIB is known to preferentially quench charge-recombination fluorescence (Booth et al., 1990), and therefore if one of the fast components is associated with charge recombination a reduction in its yield and lifetime may be expected to occur in the presence of DBMIB. However, the results obtained were inconclusive.

(*B*) *TRES.* The spectral features of fluorescence components RP-1, RP-2, and UC-1 (see Figure 7) indicate that UC-1 has a different physical origin to the two longer components. Spectrum UC-1 is clearly blue-shifted from spectra RP-1 and RP-2, consistent with the idea that the former is largely due to inactive D1/D2 reaction centers while the latter are due to charge-recombination fluorescence in active reaction centers. Other evidence that supports these assignments is as follows: (i) Charge-recombination fluorescence represented by an average of components RP-1 and RP-2 is lost as D1/D2 reaction centers are damaged, while that due to uncoupled chlorophyll increases (see Figure 2). These changes are also accompanied by an increase in the steady-state fluorescence yield and a blue-shift in the maximum of the steady-state fluorescence band (Seibert et al., 1987; Booth et al., 1990). (ii) Excellent agreement (to within ±3%) is obtained between the sample activities determined from fluorescence data, reported here, and those determined by Braun et al. (1990) using steady-state absorption spectroscopy (see Figure 3). (iii) Charge-recombination fluorescence is lost upon addition of the quinone DBMIB to D1/D2 reaction centers while that due to uncoupled chlorophyll remains unchanged (Booth et al., 1990). (iv) Other isolated higher plant chlorophyll–protein complexes that have been studied by SPC consistently show a variable amount of a component with a lifetime of approximately 6 ns that is assigned to nonfunctional chlorophyll in a protein environment or detergent micelle (Owens et al., 1987, 1988; Ide et al., 1987; Booth et al., 1990). (v) The transient absorption studies presented here.

It is difficult to obtain accurate information regarding components SH-1 and SH-2 individually, because the lifetimes and yields of these fast fluorescence components depend on the magnitude of the lifetime that represents the three longest fluorescence components during data analysis (see Analysis and Results). Nevertheless, the emission spectra that correspond to SH-1 and SH-2 can give some information as to their origins. Spectra SH-1 and SH-2 appear to be red-shifted compared to spectrum UC-1 and have maxima similar to those of components RP-1 and RP-2. However, the imprecision of the data makes it difficult to obtain the maximum wavelengths of spectra SH-1 and SH-2 accurately.

SH-2 may be due to fluorescence from P680* prior to charge separation; however, charge separation is thought to occur in D1/D2 reaction centers in approximately 3 ps (Wasielewski et al., 1989b), and any such fluorescence would be expected to have a quantum yield of $1.6 \times 10^{-4}$ (Booth et al., 1990). However, the lifetime and quantum yield (which can be calculated as $1.5 \times 10^{-3}$) of SH-2 are both an order of magnitude greater than these expected values. The lifetime of SH-2 is not resolution limited (see Materials and Methods), but it may be slightly distorted by the artificial fixing of the longest fluorescence components when analyzing data on time scale 3 (see Results).

Alternatively, SH-2 may be due to slow energy transfer to P680. Preliminary transient absorption measurements with femtosecond time resolution by our group (unpublished experiments) show an 18-ps component due to chlorophyll singlet states, which would support this assignment of SH-2. Similar observations from transient absorption measurements have been made by Wasielewski et al. (1989a).

Another possible origin of SH-1 and SH-2 is limited aggregation of D1/D2 reaction centers (see Materials and Methods). With this interpretation, the upper limit for the proportion of aggregated samples is 10–15%.

(*C*) *Transient Absorption Measurements.* The assignment of fluorescence components RP-1 and RP-2 to decay of the primary radical pair via charge recombination to P680* is confirmed by transient absorption measurements at 820 nm. Measurements at 820 nm monitor loss of $P680^+Ph^-$ and triplet P680 (Takahashi et al., 1987; Hansson et al., 1988; Schlodder & Brettel, 1988; Durrant et al., 1990). The radical pair kinetics can be adequately modeled by two or three exponentials; however, the signal to noise ratio of the absorption data is insufficient to distinguish these two models.

A lifetime of 5–6 ns, corresponding to uncoupled chlorophyll is not observed whether two or three exponentials are used to model the absorption decay. In fact, a decay kinetic associated with uncoupled chlorophyll would not be expected in these absorption studies of active D1/D2 reaction centers for the following reasons. In active D1/D2 reaction center samples, a maximum of 6% of the total chlorophyll present is nonfunctional (Booth et al., 1990; Gounaris et al., 1990). As a result, the amplitude of a component due to this nonfunctional chlorophyll would be expected to be too small to observe in our transient absorption measurements. Therefore the transient absorption measurements assign at least biexponential decay kinetics to $P680^+Ph^-$.

It is clear that whether two or three exponentials are used to model the absorption data, the longest lifetime resolved (of 54 or 56 ns, respectively) is the same as that determined by charge-recombination fluorescence measurements, where accurate resolution of the lifetimes is possible due to the better signal to noise ratio obtainable with SPC. It is also interesting to note that when three exponentials are used to model the absorption data, both of the longest lifetimes (19 and 56 ns) are identical with the longest charge-recombination fuorescence lifetimes (see Table III). In addition, a faster component is also resolved. It is entirely possible that there is such a short lifetime associated with decay of $P680^+Ph^-$, which may correspond to the fast fluorescence component, SH-1.

In summary, excellent agreement is obtained between transient absorption and fluorescence studies of $P680^+Ph^-$ decay kinetics in D1/D2 reaction centers. The time-resolved fluorescence and absorption data show that the charge-re-

combination kinetics of the primary radical pair are multiexponential and exhibit at least two components: RP-1 and RP-2. The fluorescence measurements also indicate the presence of two faster components, and the transient absorption data is also consistent with there being additional short lifetimes associated with decay of the primary radical pair. SH-1 may be associated with charge recombination of $P680^+Ph^-$ while SH-2 may result from "slow" energy transfer to P680. There is also a fluorescence component UC-1 that represents a small proportion (less than 6%) of nonfunctional chlorins.

*Proposed Models for Primary Charge Separation in D1/D2 Reaction Centers*

The multiexponential radical pair kinetics may be due to heterogeneity of D1/D2 reaction center preparations in terms of their chemical composition and stoichiometry. For example there may be small subpopulations of reaction centers that contain $Q_A$ or some antenna chlorophylls. The presence of either of these may be expected to shorten the radical pair lifetime. The observation that there are apprently six chlorophylls associated with each PS2 reaction center (Gounaris et al., 1990), as opposed to only four in the bacterial case (Deisenhofer et al., 1984), seems to imply that there may be subpopulations of "reaction centers" that do contain some antenna chlorophylls. However, there are no detectable amounts of the antenna binding 43- and 47-kDa polypeptides in D1/D2 preparations (Barber et al., 1987; Nanba & Satoh, 1987). In addition, a maximum of 2% of reaction centers in D1/D2 preparations contain plastoquinone (Chapman et al., 1991b). Therefore it is unlikely that such biochemical heterogeneity is the cause of the multiexponential kinetics.

There are several models that can explain multiexponential radical pair kinetics in terms of dynamical heterogeneity. This may be caused by parallel electron transfer along both D1 and D2 polypeptides or to equilibration of the singlet and triplet states of $P680^+Ph^-$ (Booth et al., 1990). Both of these models have been ruled out for bacterial reaction centers (Woodbury & Parson, 1984; Hörber et al., 1986; Goldstein & Boxer, 1989; Aumeier et al., 1989; Kellogg et al., 1989). Two alternative models are discussed in some detail below.

(*A*) *Sequential Relaxations of the Primary Radical Pair.* The multiexponential decay kinetics of the primary radical pair may be due to quasistatic equilibria between P680* and radical pair states that are formed sequentially as a result of relaxations. Assuming that the decay kinetics are represented by three exponentials corresponding to three radical pair states with different free energies, then the radical pair is initially formed with a free energy of approximately 0.05 eV below P680* (for the first 500 ps) and then relaxes to a state 0.116 eV below P680* (for about 20 ns) and finally to a state 0.143 eV below P680* (which lives for 52 ns) (see Appendix B for details of these free energy calculations). It is possible that rather than three discrete radical pair states the decay may actually represent a continuous relaxation process whereby the free energy of the primary radical pair changes continuously over nanoseconds. This would result in the "equilibrium" ($P680^* \rightleftharpoons P680^+Ph^-$) and the radical pair lifetime changing continuously with time. In this case invoking quasistatic equilibria on time scales of 500 ps and 20 ns is invalid; however, the free energy calculation for formation of the final radical pair, with a 52-ns lifetime, still holds.

There is some evidence for relaxations of $P680^+Ph^-$ from studies of larger PS2 preparations that contain antenna chlorophylls (Schlodder & Brettel, 1988; Takahashi et al., 1987; Schatz et al., 1987; Hansson et al., 1988; Holzwarth, 1989). Lifetimes ranging from 2 to 25 ns have been reported for $P680^+Ph^-$ and have been tentatively assigned to varying structural relaxations in the radical pair after its formation; however, they may equally well be due to different experimental conditions (Takahashi et al., 1987; Hansson et al., 1988). More convincing evidence for relaxations occurring in the radical pair state in PS2 comes from the temperature dependence of the radical pair kinetics in PS2 particles from *Synechococcus* (Schlodder & Brettel, 1988, 1990). At room temperature single-exponential kinetics were observed, while at temperatures of 80 and 5 K the decay of the radical pair was clearly biexponential. The authors interpreted these results as evidence that the radical pair exists in different conformations.

A sequential relaxation mechanism appears to be the one most favored for bacterial reaction centers (Woodbury & Parson, 1984; Goldstein & Boxer, 1989; Ogrodnik, 1990).

(*B*) *Conformational Substates of Reaction Centers.* Since the chromophores involved in electron transfer are bound to a protein complex, it is possible that the multiexponential decay kinetics arise from conformational heterogeneity of the protein. Such heterogeneity could arise from differences in side-chain arrangement, hydrogen bonds, and the relative distance/orientation of the cofactors. This sort of structural heterogeneity in the chromophore environment will cause otherwise identical chromophores to decay at slight different rates. The effect on the observed kinetics will depend on the time scale of the interconversion between conformational substates. In this model the observation of two (or more) lifetimes associated with $P680^+Ph^-$ decay implies that there are at least two discrete conformational substates of the protein that interconvert on a time scale longer than tens of nanoseconds. These two substates cause $P680^+Ph^-$ to decay at slightly different rates of 20 and 52 ns. In addition there may also be a third substate that is associated with SH-1. These substates could be present prior to excitation of P680 so that independent ($P680^* \rightleftharpoons P680^+Ph$) equilibria are established. Alternatively, the conformational heterogeneity may be induced on radical pair formation with no such heterogeneity existing in the P680* state. It may be that formation of $P680^+Ph^-$ results in access to two, or more, conformers of the protein as a result of a change in electrostatic interactions or by restricting side-chain motion.

It is possible that there are far more than just two substates of the protein, there could be several different conformers that decay with lifetimes of the order of 20 ns (or rapidly interconvert with each other on time scales less than 20 ns) and several that decay with lifetimes in the region of 52 ns. This would lead to a distribution of lifetimes centered on 20 and 52 ns that would not be resolved when fitting the data to a sum of only a few exponentials. An attempt has been made to analyze fluorescence kinetics of D1/D2 reaction centers by using a continuous distribution of exponentials (Govindjee et al., 1990), but this type of analysis does not take into account specific contributions to the kinetics, for example, from inactive reaction centers. The model proposed here would result in discrete distributions of exponentials centered on 5, 20, and 52 ns, rather than a continuous distribution.

The data presented in Figure 5 are calculated for the conformational substate model without taking into account SH-1. To incorporate SH-1 into the calculations of $\Delta G_{RP\text{-}1}$ and $\Delta G_{RP\text{-}2}$, accurate transient absorption data on SH-1 are required. Although this is beyond the time resolution of the absorption experiments described here, it is possible to estimate the effect of SH-1 on these free energy calculations (see Appendix B): only the magnitudes of $\Delta G_{RP\text{-}1}$ and $\Delta G_{RP\text{-}2}$ are

slightly reduced while their temperature dependence remains the same as in Figure 5.

Distributions of conformational substates have been widely discussed in relation to globular proteins such as myoglobin and haemoglobin (Beece et al., 1980; Elber & Karplus, 1987; Frauenfelder et al., 1988). For example, ligand-binding studies of myoglobin have indicated that this protein exists in at least three major conformational substates that perform identical functions but with different kinetics (Hong et al., 1990). There is also evidence that bacterial reaction centers may exist in different conformations. This comes from the observation of a spread in rates of primary and secondary charge separation (Kirmaier & Holten, 1990) and of multiexponential charge-recombination kinetics of $P^+Q_A^-$ (Kleinfeld et al., 1984; Baciou et al., 1990; Gao et al., 1991). There is also some evidence that such conformational heterogeneity may exist in PS2 preparations. The observation of multiexponential charge-recombination kinetics of $P680^+Q_A^-$ in oxygen-evolving PS2 preparations from *Synechococcus* have been assigned to a distribution of structural states of the reaction center proteins (Gerken et al., 1989). In addition, the results discussed above in relation to the sequential relaxation model, concerning the observation of monoexponential radical pair kinetics that become biexponential at low temperatures (Schlodder & Brettel, 1988, 1990), also may be a result of conformational heterogeneity of the reaction center proteins.

*Entropy Contribution to $\Delta G(P680^+Ph^- - P680^*)$*

A previous paper has reported the temperature dependence of the average free energy of formation of the primary radical pair in D1/D2 reaction centers, calculated from monoexponential decay kinetics of the primary radical pair with a lifetime of 37 ns (Booth et al., 1990). This free energy change had a linear temperature dependence from 220 to 77 K, indicating that over this temperature range the free energy change was dominated by entropy. Figure 5 shows that $\Delta G_{RP\text{-}1}$ and $\Delta G_{RP\text{-}2}$ exhibit similar temperature dependences to this average free energy change; therefore, the conclusions reported by Booth et al. (1990) are still valid.

The entropy change for charge separation is found from the gradient over the linear region of the $\Delta G$ curve ($\Delta G = \Delta H - T\Delta S$). Therefore the free energies of formation of both radical pair states RP-1 and RP-2 appear to be dominated by entropy from 77 to 230 K, with the enthalpy contribution being negligible. The results also suggest that the difference in states RP-1 and RP-2 is enthalpic.

The observation of a linear region in the $\Delta G$ curve over a significant temperature range indicates that both $\Delta S$ and $\Delta H$ are temperature independent. Any temperature dependence of these terms will cause a deviation from linearity. For example, the temperature dependences of the entropy and enthalpy changes between different substates of myoglobin introduces a quadratic dependence of $\Delta G$ on temperature, $\Delta G = \Delta H - T\Delta S - {}^1/_2\Delta s T^2$ (Hong et al., 1990). From 230 to 293 K, the temperature dependence of $\Delta G$ is nonlinear (see Figure 5). This could imply that enthalpy and/or entropy are (is) temperature dependent in this region, and therefore it is impossible to deduce values for the entropy and enthalpy contributions to $\Delta G$ over this temperature range. The exact cause of this nonlinearity is unknown, but it may be connected with a phase change of D1/D2 reaction center samples. Alternatively, it is possible that rapid unresolved relaxations of the radical pair may occur over this temperature range or that one or more intermediate states are trapped at this temperature.

The entropy change can be thought of as a change in the vibrational entropy of the reacting system, this includes any changes as a result of "rotations" of any side groups of the protein. Vibrational entropy depends on two things: (i) the total number of vibrational states or modes that can be occupied (density of states); (ii) the total number of phonons available to occupy these states. An increase in entropy can therefore result from an increase in either the density of states or the number of phonons. The latter occurs when a high-energy vibrational phonon breaks down into several phonons of smaller energy. This means that primary electron transfer has to occur from vibrationally excited P680*. The entropy can also increase through an increase in the density of vibrational states (Kakitani & Kakitani, 1981). This can be thought of as a change in curvature of the potential energy surfaces of the reactant and product states. If the product state has a shallower curvature compared to the reactant state, then more vibrational states will be available for occupation at any one temperature. Instead of a large entropy change being associated with a single vibrational mode, it is possible that such a contribution to the entropy change on electron transfer could be caused by structural changes that affect several vibrational modes, with each mode experiencing only small changes. The temperature dependence of secondary electron transfer, from $Ph^-$ to $Q_A$, in *Rb. sphaeroides* reaction centers has been interpreted by using a model that involves a change in the density of vibrational states on electron transfer (Kirmaier et al., 1985). Fitting the data to such a model indicated that there was an increase in entropy on electron transfer.

Another contribution to the entropy change could be due to varying degrees of anharmonicity in the reactant and product potential energy surfaces. These different degrees of anharmonicity would result in different vibrational level spacing and therefore different densities of vibrational states for the reactants and products.

The entropy change could also be interpreted in terms of the conformational substate model. If there are more conformers associated with the radical pair state than P680*, then the entropy would be expected to increase on charge separation, due to the increase in the number of possible protein configurations. The difference between protein conformers could be due to several factors, such as hydrogen bonding, side-chain rearrangement, and relative chromophore position, which may be altered on formation of $P680^+Ph^-$. Computer simulations of primary electron transfer in bacterial reaction centers have indicated that electron transfer may be accompanied by rearrangements of dipolar side groups of the protein and of the primary acceptor pheophytin (Treutlein et al., 1988).

*Comparison with Bacterial Reaction Centers*

The reaction centers of PS2 and purple bacteria are thought to be structurally analogous, particularly regarding those chromophores involved in primary charge separation (Trebst, 1986; Barber, 1987, Michel & Deisenhofer, 1988). There are also some similarities in the kinetics of the two systems. In both cases, multiexponential fluorescence kinetics are observed. In *Rb. sphaeroides* and *Rps. viridis* reaction centers, at least three fluorescence components have been reported with lifetimes of approximately 12, 2, and 0.2 ns (Woodbury & Parson, 1984; Hörber et al., 1986). At present, a model is favored where these lifetimes are assigned to charge-recombination fluorescence from the primary radical pair, with the different lifetimes reflecting relaxations in the free energy of the radical pair (Woodbury & Parson, 1984; Goldstein & Boxer, 1989; Ogrodnik, 1990), as under Sequential Reactions of the Primary Radical Pair above. In transient absorption studies of *Rb.*

Table AI: Analysis of Simulated Fluorescence Decays

| | simulated decay | | analyzed output | |
|---|---|---|---|---|
| data set | $\tau$ (ns)[a] | $F$ (%)[b] | $\tau$ (ns)[a] | $F$ (%)[b] |
| 1 | 35.0 | 7.9 | 33.0 | 6.4 |
| | 5.5 | 66.1 | 5.5 | 67.7 |
| | 1.3 | 26.0 | 1.3 | 25.9 |
| 2 | 35.0 | 5.2 | 19.8 | 3.4 |
| | 5.5 | 68.1 | 5.5 | 67.7 |
| | 1.3 | 26.7 | 1.3 | 28.9 |
| 3 | 35.0 | 3.5 | 1.5 | 0.6 |
| | 5.5 | 69.3 | 5.7 | 71.0 |
| | 1.3 | 27.2 | 1.4 | 27.5 |
| 4 | 35.0 | 1.2 | 17.8 | 0.1 |
| | 5.5 | 70.9 | 5.5 | 72.9 |
| | 1.3 | 27.9 | 1.3 | 27.0 |
| 5 | 35.0 | 1.0 | negative | 2940 |
| | 5.5 | 71.1 | ≈72 | 5.5 |
| | 1.3 | 27.9 | ≈28 | 1.3 |

[a] Lifetime. [b] Relative yield.

*sphaeroides* reaction centers only the slowest component (12 ns) has been observed (Schenck et al., 1982; Chidsey et al., 1984).

This paper reports multiexponential charge-recombination fluorescence kinetics for D1/D2 reaction centers, but in contrast to the bacterial case the same lifetimes are seen in both transient absorption and fluorescence studies. In fact this is the first time that agreement has been demonstrated between transient absorption and fluorescence kinetics of a reaction center. The difference between the bacterial and PS2 cases may indicate a genuine difference between the radical pair behavior. Alternatively, it may reflect the difficulties associated with obtaining sufficiently high signal to noise data, combined with appropriate analysis.

Two methods have been used to determine the free energy of primary charge separation in bacterial reaction centers: time-resolved fluorescence measurements (Woodbury & Parson, 1984; Hörber et al., 1986) and magnetic field dependent studies of triplet special pair, $^3$P, kinetics (Goldstein et al., 1988; Ogrodnik et al., 1988). The fluorescence studies of Woodbury and Parson imply that the free energy of charge separation is dominated by entropy. In contrast, the magnetic field studies of $^3$P imply that this free energy is dominated by enthalpy, with a negligible entropy contribution (Goldstein et al., 1988; Ogrodnik et al., 1988). This paradox has not been satisfactorily explained. However, several factors have to be considered before making a direct comparison of these results: the studies were over different temperature ranges and under different experimental conditions. In addition, the conclusions from the magnetic field studies require a detailed knowledge of the reaction scheme within bacterial reaction centers, while interpretation of fluorescence data does not. The reaction scheme used for analysis of the magnetic field data has since been shown to be incomplete (Goldstein & Boxer, 1989). The magnetic field measurements were made on a different time scale to the fluorescence measurements, microseconds as opposed to nanoseconds, and it has been suggested that the two experiments probe relaxed and unrelaxed states, respectively, of the reaction center and hence the radical pair (Woodbury & Parson, 1984; Ogrodnik et al., 1988; Goldstein & Boxer, 1989). However, this does not explain the difference in the entropy and enthalpy contributions. It is possible to estimate the temperature dependence of the free energy of formation of the relaxed radical pair state from 77 to 290 K from Woodbury and Parson's data (Booth, 1990). Such an estimation also indicates that the free energy of formation of a relaxed radical pair is also dominated by entropy, in contrast to the conclusions of the magnetic field data.

Table AII: Analysis of a Simulated Data Set on Time Scale 2

| simulated decay | | analyzed output | |
|---|---|---|---|
| $\tau$ (ns) | $F$ (%) | $\tau$ (ns) | $F$ (%) |
| 52.0 | 34.6 | 36.9 | 45.3 |
| 17.0 | 16.7 | | |
| 6.0 | 37.2 | 6.0 | 44.2 |
| 1.5 | 6.9 | 1.1 | 7.1 |
| 0.5 | 4.6 | 0.5 | 3.4 |

For simplicity, several interpretations of experimental data on primary electron transfer have assumed that the free energy of charge separation is dominated by enthalpy (Jortner, 1980; Fleming et al., 1988), an approach consistent with the magnetic field results. The surprising similarity of the temperature dependence of the free energy of primary charge separation in bacterial and D1/D2 reaction centers, presented in this paper (see Figure 5), strongly supports Woodbury and Parson's observations: the free energy of formation of both radical pair states RP-1 and RP-2 in PS2 reaction centers appears to be dominated by entropy. Therefore the entropy contribution to the free energy of charge separation cannot be assumed to be negligible.

## Conclusion

The primary radical pair in D1/D2 reaction centers exhibits multiexponential decay kinetics. The exact number and values of lifetimes assigned to $P680^+Ph^-$ decay are less illuminating than the fact that the radical pair lifetime is not monoexponential; indeed, the decay may actually reflect a distribution of components. The different exponential components may be due to equilibria between P680* and different radical pair states caused by a dynamic distribution of reaction center structures, possibly due to different conformations of the protein or to an initial radical pair state that relaxes to another state (or states) of lower energy. Whichever model is used to interpret the decay kinetics, formation of both radical pair states appears to be dominated by entropy over a large temperature range.

It is necessary to consider how information on the radical pair states (on a nanosecond time scale) can be related to the primary electron transfer step itself, which occurs in a few picoseconds. Since the properties of the primary radical pair appear to be time dependent, it is difficult to obtain the appropriate free energy that acts as the driving force for the picosecond primary electron transfer step. It is possible that the entropy change that apparently dominates the free energy of formation of the radical pair states is not the driving force for the electron transfer reaction itself, but is a result of nuclear relaxations immediately after electron transfer that reduce the amount of charge recombination. The role of structural changes in enhancing charge stabilization in this manner has previously been suggested by Kleinfeld et al. (1984).

## Acknowledgments

We thank Niall Walsh for preparation of the D1/D2 reaction centers and Dr. Chris Barnett for overall technical assistance. We also thank Drs. James Durrant and David Chapman for helpful discussions and Martin Bell for assistance with data analysis.

## Appendix A

### *Simulated Data Studies*

*(A) Magnitude of Charge-Recombination Fluorescence Lifetime on Reaction Center Degradation.* Simulated

fluorescence decays were created on time scale 2 with variable amounts of a 35-ns component (see Table AI, columns two and three). The results of analyzing these decays to three exponentials with all parameters free running are also shown in Table AI. Comparing the results of this simulated data study to those in Table II shows that the analysis of fluorescence decays 4 and 5 of Table II are consistent with there being approximately 5% and 1% of a 37-ns component, respectively (cf. data sets sets 2 and 5 in Table AI).

*(B) Resolution of 20-ns and 52-ns Lifetimes on Time Scale 2.* A simulated fluorescence decay was created on time scale 2, with 20000 CPC and consisting of a 17-ns and a 52-ns component (see Table AII, columns one and two). The results of analyzing this decay are also shown in Table AII. Although the simulated decay consists of 17-ns and 52-ns lifetimes, the analysis software consistently and incorrectly resolves these as a single lifetime of 37 ns.

## Appendix B

It is possible to calculate the equilibrium constant $K$ for the primary charge separation equilibrium

$$P680^* \rightleftharpoons P680^+Ph^- \quad (1)$$

from time-resolved fluorescence measurements by using

$$K = \frac{[P680^+Ph^-]_e}{[P680^*]_e} = \frac{A(P^*_i)}{A(P^*_e)} \quad (2)$$

where $A(P^*_i)$ and $A(P^*_e)$ are the initial amplitudes of the fluorescence decays from P680* initially (before the equilibrium is established) and at equilibrium, respectively. If the equilibrium in eq 1 decays with a single-exponential lifetime, then $K$ is found from (Booth et al., 1990)

$$K = \frac{\int_0^\infty \exp(-t/\tau_1)}{\phi_1 \int_0^\infty \exp(-t/\tau_0)} = \frac{\tau_1}{\phi_1 \tau_0} \quad (3)$$

where $\tau_1$ is the lifetime of charge-recombination fluorescence, $\phi_1$ is the quantum yield of charge-recombination fluorescence, and $\tau_0$ is the natural lifetime of P680* [which is taken as 19 ns (Booth et al., 1990)]. The free energy of primary charge separation, $\Delta G(P680^+Ph^- - P680^*)$, is calculated from $K$ by using

$$\Delta G = -k_B T \ln K \quad (4)$$

where $\Delta G$ is the standard free energy change per molecule and $k_B$ is the Boltzmann constant. In a previous paper, $\Delta G(P680^+Ph^- - P680^*)$ was calculated for D1/D2 reaction centers from time-resolved fluorescence measurements made on time scale 2 (Booth et al., 1990). When a value of 37 ns for $\tau_1$ was used, $\Delta G(P680^+Ph^- - P680^*)$ was found to be −0.11 eV. However, since this lifetime is really an average of (at least) two lifetimes of 20 and 52 ns, the calculated free energy gap of −0.11 eV also represents an average free energy of formation of the primary radical pair.

*(A) Sequential Relaxation Model.* In this model, eq 3 can still be used to calculate $K_{RP\text{-}1}$. The calculation of $K$ from eq 3 assumes that the concentration of $P680^+Ph^-$ at equilibrium is essentially equal to the concentration of P680* initially, before any radical pair formation.

In eq 3 the initial fluorescence amplitude of P680* at equilibrium is found from the initial amplitude of the charge-recombination fluorescence component with lifetime $\tau_1$. If, however, the radical pair state formed on a 20-ns time scale then relaxes to another radical pair state (which is formed on a 52-ns time scale) so that two radical pair states are formed sequentially, eq 3 does not apply to the calculation of $K$ on a time scale of 20 ns. In this case, the initial amplitude of P680* for the quasistatic equilibrium that is established in 20 ns has to be found from the sum of the initial amplitudes of both the 20-ns and 52-ns fluorescence components:

$$A(P^*_e) = \frac{\phi_1}{\int_0^\infty \exp(-t/\tau_1)} + \frac{\phi_2}{\int_0^\infty \exp(-t/\tau_2)} = (\phi_1/\tau_1) + (\phi_2/\tau_2) \quad (5)$$

and $K$ is calculated from

$$K_2 = \frac{1/\tau_0}{(\phi_1/\tau_1) + (\phi_2/\tau_2)} \quad (6)$$

where $\tau_2$ and $\phi_2$ are the lifetime and quantum yield of RP-2 and $\tau_1$ and $\phi_1$ are the corresponding parameters for RP-1.

Similarly, for the calculation of $K$ for formation of a radical pair state on a 500-ps time scale

$$A(P^*_e) = (\phi_1/\tau_1) + (\phi_2/\tau_2) + (\phi_3/\tau_3) \quad (7)$$

$$K_3 = \frac{1/\tau_0}{(\phi_1/\tau_1) + (\phi_2/\tau_2) + (\phi_3/\tau_3)} \quad (8)$$

where $\tau_3$ and $\phi_3$ are the lifetime and quantum yield of SH-1. Incorporating SH-1 in this model has no effect on the calculations of $K_{RP\text{-}1}$ and $K_{RP\text{-}2}$.

If quasistatic equilibria cannot be invoked on time scales of 500 ps and 20 ns, then eqs 5–8 are invalid; however, the calculation of $K_{RP\text{-}1}$ still holds.

*(B) Conformational Substate Model.* In the simplest form of this model, the reaction centers exist in two conformational states that interconvert on a time scale longer than tens of nanoseconds, with the radical pair states of the two conformers decaying monoexponentially with different lifetimes of 20 and 52 ns. This means there are two independent ($P680^* \rightleftharpoons P680^+Ph^-$) equilibria. Equation 3 can be used to calculate $K$ for both equilibria; however, the relative proportions of $P680^+Ph^-$ involved in the two equilibria have to be taken into account. The transient absorption data indicate that there is approximately twice as much of radical pair RP-1 as RP-2 (see Table III). Therefore, the equilibrium constants can be calculated from

$$K' = c\frac{\tau_1}{\phi_1 \tau_0} \quad (9)$$

where $c$ is the proportion of $P680^+Ph^-$ involved in the equilibrium. At 293 K, $K_{RP\text{-}2}$ is calculated with $c = {}^1/_3$, $\tau_1 = 20$, and $\phi_1 = 0.72$, while $K_{RP\text{-}1}$ is calculated with $c = {}^2/_3$, $\tau_1 = 52$, and $\phi_1 = 0.94$. The temperature dependences of $\Delta G_{RP\text{-}1}$ and $\Delta G_{RP\text{-}2}$ given in Table IV and Figure 5 were determined on the basis that these $c$ values do not change with temperature.

Incorporating a third conformer in this model, which has a radical pair state that decays with a 500-ps lifetime, alters the value of $c$ in eq 9. The transient absorption data shown in Table III allow rough estimates of the relative proportions of $P680^+Ph^-$ involved in the three ($P680^* \rightleftharpoons P680^+Ph^-$) equilibria. The equilibrium constant for the 500-ps radical pair is calculated with $c = {}^2/_5$, $K_{RP\text{-}2}$ is calculated with $c = {}^1/_5$, and $K_{RP\text{-}1}$ is calculated with $c = {}^2/_5$. Therefore the magnitudes of $K_{RP\text{-}1}$, $K_{RP\text{-}2}$, $\Delta G_{RP\text{-}1}$, and $\Delta G_{RP\text{-}2}$ are reduced. The 500-ps component was not included in the calculations

given in Table IV and Figure 5 because of the uncertainty associated with the transient absorption data of this component and with its physical origin.

## References


Aumeier, W., Eberl, U., Ogrodnik, A., Volk, M., Scheidel, G., Feick, R., Plato, M., & Michel-Beyerle, M. E. (1990) in *Current Research in Photosynthesis* (Baltscheffsky, M., Ed.) Vol. I, pp 133–136, Kluwer, Dordrecht.

Baciou, L., Rivas, E., & Sebban, P. (1990) *Biochemistry 29*, 2966–2976.

Barber, J. (1987) *Trends Biochem. Sci. 12*, 321–326.

Barber, J., Chapman, D. J., & Telfer, A. (1987) *FEBS Lett. 220*, 67–73.

Beece, D., Eisenstein, L., Fraunefelder, H., Good, D., Marden, M. C., Reinisch, L., Reynolds, A. H., Sorensen, L. B., & Yue, K. T. (1980) *Biochemistry 19*, 5147–5157.

Bixon, M., Jortner, J., Michel-Beyerle, M. E., & Ogrodnik, A. (1989) *Biochim. Biophys. Acta 977*, 273–286.

Booth, P. J. (1990) Ph.D. Thesis, University of London.

Booth, P. J., Crystall, B., Giorgi, L. B., Barber, J., Klug, D. R., & Porter, G. (1990) *Biochim. Biophys. Acta 1016*, 141–152.

Braun, P., Greenberg, B. M., & Scherz, A. (1990) *Biochemistry 29*, 10376–10387.

Chapman, D. J., Gounarus, K., & Barber, J. (1988) *Biochim. Biophys. Acta 933*, 423–431.

Chapman, D. J., Gounaris, K., & Barber, J. (1989) *Photosynthetica 23*, 411–426.

Chapman, D. J., Gounaris, K., & Barber, J. (1991a) in *Plant Biochemistry Amino Acids, Proteins and Nucleic Acids* (Rogers, L. J., Ed.) Vol. 5, pp 171–193, Academic Press, London.

Chapman, D. J., Vass, I., & Barber, J. (1991b) *Biochim. Biophys. Acta 1057*, 391–398.

Chidsey, C. E. D., Kirmaier, C., Holten, D., & Boxer, S. G. (1984) *Biochim. Biophys. Acta 766*, 424–437.

Crystall, B., Booth, P. J., Klug, D. R., Barber, J., & Porter, G. (1989) *FEBS Lett. 249*, 75–78.

Danielius, R. V., Satoh, K., van Kan, P. J. M., Plijter, J. J., Nuijs, A. M., & van Gorkom, H. J. (1987) *FEBS Lett. 213*, 241–244.

Deisenhofer, J., Epp, O., Miki, K., Huber, R., & Michel, H. (1984) *J. Mol. Biol. 180*, 385–398.

Durrant, J. R., Giorgi, L. B., Barber, J., Klug, D. R., & Porter, G. (1990) *Biochim. Biophys. Acta 1017*, 167–175.

Elber, R., & Karplus, M. (1987) *Science 235*, 318–321.

Fleming, G. R., Martin, J. L., & Breton, J. (1988) *Nature 333*, 190–192.

Frauenfelder, H., Parak, F., & Young, R. D. (1988) *Annu. Rev. Biophys. Biophys. Chem. 17*, 451–479.

Fujita, I., Davis, M. S., & Fajer, J. (1978) *J. Am. Chem. Soc. 100*, 6280–6282.

Gao, J.-L., Shapes, R. J., & Wraight, C. A. (1991) *Biochim. Biophys. Acta 1056*, 259–272.

Gerken, S., Dekker, J. P., Schlodder, E., & Witt, H. T. (1989) *Biochim. Biophys. Acta 977*, 52–61.

Goldstein, R. A., & Boxer, S. G. (1989) *Biochim. Biophys. Acta 977*, 78–86.

Goldstein, R. A., Takiff, L., & Boxer, S. G. (1988) *Biochim. Biophys. Acta 934*, 253–263.

Gounaris, K., Chapman, D. J., Booth, P., Crystall, B., Giorgi, L. B., Klug, D. R., Porter, G., & Barber, J. (1990) *FEBS Lett. 265*, 88–92.

Govindjee, van de Ven, M., Preston, C., Seibert, M., & Gratton, E. (1990) *Biochim. Biophys. Acta 1015*, 173–179.

Hansson, Ö., Duranton, J., & Mathis, P. (1988) *Biochim. Biophys. Acta 932*, 91–96.

Holzapfel, W., Finkele, U., Kaiser, W., Osterhelt, D., Scheer, H., Stilz, H. U., & Zinth, W. (1990) *Proc. Natl. Acad. Sci. U.S.A. 87*, 5168–5172.

Holzwarth, A. R. (1989) *Q. Rev. Biophys. 22*, 239–326.

Hong, M. K., Braunstein, D., Cowen, B. R., Fraunefelder, H., Iben, I. E. T., Mourant, J. R., Ormas, P., Scholl, R., Schulte, A., Steinbach, P. J., Xie, A.-H., & Young, R. D. (1990) *Biophys. J. 58*, 429–436.

Hörber, J. K. H., Göbel, W., Ogrodnik, A., Michel-Beyerle, M. E., & Cogdell, R. J. (1986) *FEBS Lett. 198*, 273–278.

Ide, J. P., Klug, D. R., Kühlbrandt, W., Giorgi, L. B., & Porter, G. (1987) *Biochim. Biophys. Acta 893*, 349–364.

Ikeuchi, M., & Inoue, Y. (1988) *FEBS Lett. 241*, 99–104.

Jortner, J. (1980) *J. Am. Chem. Soc. 102*, 6676–6686.

Kakitani, T., & Kakitani, H. (1981) *Biochim. Biophys. Acta 635*, 498–514.

Kellogg, E. C., Kolaczkowski, S., Wasielewski, M. R., & Tiede, D. M. (1989) *Photosynth. Res. 22*, 47–59.

Kirmaier, C., & Holten, D. (1987) *Photosynth. Res. 13*, 225–260.

Kirmaier, C., & Holten, D. (1990) *Proc. Natl. Acad. Sci. U.S.A. 87*, 3552–3556.

Kirmaier, C., Holten, D., & Parson, W. W. (1985) *Biochim. Biophys. Acta 810*, 33–48.

Kleinfeld, D., Okamura, M. Y., & Feher, G. (1984) *Biochemistry 23*, 5780–5786.

Knutson, J. R., Beecham, J. M., & Brand, L. (1983) *Chem. Phys. Lett. 102*, 501–507.

Marcus, R. A. (1990) in *Current Research in Photosynthesis* (Baltscheffsky, M., Ed.) Vol. I, pp 1–10, Kluwer, Dordrecht.

Marcus, R. A., & Sutin, N. (1985) *Biochim. Biophys. Acta 811*, 265–322.

Marquardt, D. W. (1963) *J. Soc. Ind. Appl. Math. 11*, 431–441.

Mathis, P., & Setif, P. (1981) *Isr. J. Chem. 21*, 316–320.

Mathis, P., Satoh, K., & Hansson, O. (1989) *FEBS Lett. 251*, 241–244.

McTavish, H., Picorel, R., & Seibert, M. (1989) *Plant Physiol. 89*, 452–456.

Michel, H., & Deisenhofer, J. (1988) *Biochemistry 27*, 1–7.

Mimuro, M., Yamazaki, I., Itoh, S., Tamai, N., & Satoh, K. (1988) *Biochim. Biophys. Acta 933*, 478–486.

Nanba, O., & Satoh, K. (1987) *Proc. Natl. Acad. Sci. U.S.A. 84*, 109–112.

O'Connor, D. V., & Phillips, D. (1984) *Time-Correlated Single Photon Counting*, Academic Press, London.

Ogrodnik, A. (1990) *Biochim. Biophys. Acta 1020*, 65–71.

Ogrodnik, A., Volk, M., Letterer, R., Feick, R., & Michel-Beyerle, M. E. (1988) *Biochim. Biophys. Acta 936*, 361–371.

Owens, T. G., Webb, S. P., Mets, L., Alberte, R. S., & Felming, G. R. (1987) *Proc. Natl. Acad. Sci. U.S.A. 84*, 1532–1536.

Owens, T. G., Webb, S. P., Alberte, R. S., Mets, L., & Fleming, G. R. (1988) *Biophys. J. 53*, 733–745.

Parson, W. W., Chu, Z.-T., & Warshell, A. (1990) *Biochim. Biophys. Acta 1017*, 251–272.

Roelofs, T. A., & Holzwarth, A. R. (1990) *Biophys. J. 57*, 1141–1153.

Schatz, G. H., Brock, H., & Holzwarth, A. R. (1987) *Proc. Natl. Sci. U.S.A. 84*, 8414–8418.

Schenck, C. C., Blankenship, R. E., & Parson, W. W. (1982) *Biochim. Biophys. Acta 680*, 44–59.

Schlodder, E., & Brettel, K. (1988) *Biochim. Biophys. Acta 933*, 22-34.
Schlodder, E., & Brettel, K. (1990) in *Current Research in Photosynthesis* (Baltscheffsky, M., Ed.) Vol. I, pp 447-450, Kluwer, Dordrecht.
Seibert, M., Picorel, R., Rubin, A. B., & Connolly, J. S. (1988) *Plant. Physiol. 87*, 303-306.
Shipton, C. A., & Barber, J. (1991) *Proc. Natl. Acad. Sci. U.S.A.* (in press).
Takahashi, Y., Hansson, Ö., Mathis, P., & Satoh, K. (1987) *Biochim. Biophys. Acta 893*, 49-59.
Tetenkin, V. L., Gulyaev, B. A., Seibert, M., & Rubin, A. B. (1989) *FEBS Lett. 250*, 459-463.
Trebst, A. (1986) *Z. Naturforsch. 41c*, 240-245.
Treutlein, H., Schulten, K., Niedermeier, C., Deisenhofer, J., Michel, H., & DeVault, D. (1988) in *The Purple Bacterial Reaction Center: Structure and Dynamics* (Breton, J., & Verméglio, A., Eds.) pp 369-377, Plenum Press, New York.
Wasielewski, M. R., Johnson, D. G., Govindjee, Preston, C., & Seibert, M. (1989a) *Photosynth. Res. 22*, 89-99.
Wasielewski, M. R., Johnson, D. G., Seibert, M., & Govindjee (1989b) *Proc. Natl. Acad. Sci. U.S.A. 86*, 524-528.
Webber, A. N., Packman, L., Chapman, D. J., Barber, J., & Gray, J. C. (1989) *FEBS Lett. 242*, 259-262.
Woodbury, N. W. T., & Parson, W. W. (1984) *Biochim. Biophys. Acta 767*, 345-361.

# Photoinhibition of Hydroxylamine-Extracted Photosystem II Membranes: Identification of the Sites of Photodamage†

Danny J. Blubaugh,‡,§ Mike Atamian,∥ Gerald T. Babcock,∥ John H. Golbeck,⊥ and George M. Cheniae*,‡
*University of Kentucky, Lexington, Kentucky 40546-0091, Department of Chemistry, Michigan State University, East Lansing, Michigan 48824, and Department of Biochemistry, University of Nebraska, Lincoln, Nebraska 68583-0718*
*Received December 28, 1990; Revised Manuscript Received May 8, 1991*

ABSTRACT: Electron paramagnetic resonance (EPR) analyses ($g = 2$ region) and optical spectrophotometric analyses of $P_{680}^+$ were made of $NH_2OH$-extracted photosystem II (PSII) membranes after various durations of weak-light photoinhibition, in order to identify the sites of damage responsible for the observed kinetic components of the loss of electron transport [Blubaugh, D. J., & Cheniae, G. M. (1990) *Biochemistry 29*, 5109-5118]. The EPR spectra, recorded in the presence of $K_3Fe(CN)_6$, gave evidence for rapid ($t_{1/2}$ = 2-3 min) and slow ($t_{1/2}$ = 3-4 h) losses of formation of the tyrosyl radicals $Y_Z^+$ and $Y_D^+$, respectively, and the rapid appearance ($t_{1/2}$ = 0.8 min) of a 12-G-wide signal, centered at $g = 2.004$, which persisted at 4 °C in subsequent darkness in rather constant abundance ($\sim^1/_2$ spin per PSII). This latter EPR signal is correlated with quenching of the variable chlorophyll *a* fluorescence yield and is tentatively attributed to a carotenoid (Car) cation. Exogenous reductants ($NH_2OH \geq NH_2NH_2 > DPC \gg Mn^{2+}$) were observed to reduce the quencher, but did not reverse other photoinhibition effects. An additional 10-G-wide signal, tentatively attributed to a chlorophyll (Chl) cation, is observed during illumination of photoinhibited membranes and rapidly decays following illumination. The amplitude of formation of the oxidized primary electron donor, $P_{680}^+$, was unaffected throughout 120 min of photoinhibition, indicating no impairment of charge separation from $P_{680}$, via pheophytin (Pheo), to the first stable electron acceptor, $Q_A$. However, a 4-$\mu$s decay of $P_{680}^+$, reflecting $Y_Z \rightarrow P_{680}^+$, was rapidly ($t_{1/2}$ = 0.8 min) replaced by an 80-140-$\mu$s decay, presumably reflecting $Q_A^-/P_{680}^+$ back-reaction. Photoinhibition caused no discernible decoupling of the antenna chlorophyll from the reaction center complex. We conclude that the order of susceptibility of PSII components to photodamage when $O_2$ evolution is impaired is $Chl/Car > Y_Z > Y_D \gg P_{680}$, Pheo, $Q_A$.

Photosystem II (PSII)[1] is a large membrane-bound multiprotein complex that photochemically catalyzes the oxidation of water and the reduction of plastoquinone. Its reaction center (RC) consists of a heterodimer of homologous polypeptides, $D_1$ and $D_2$, which together contain the primary electron donor chlorophyll(s) ($P_{680}$), the secondary electron donor tyrosines $Y_Z$ and $Y_D$ of $D_1$ and $D_2$, respectively, the intermediate electron acceptor to $P_{680}$, pheophytin (Pheo), and the primary ($Q_A$) and secondary ($Q_B$) plastoquinone electron acceptors, along with an associated non-heme Fe. Closely associated with the RC is cyt *b*-559, the function of which is not clear. Light

† This work was supported principally by the U.S. Department of Energy (Contract DE-FG05-86ER13533 to G.M.C.) and partially by the USDA Competitive Research Grants Office, Photosynthesis Program (90-37262-5701 to G.T.B.), and the National Science Foundation (NSF DMB-8905065 to J.H.G.). A portion of this work was presented at the VIIIth International Congress on Photosynthesis (Blubaugh & Cheniae, 1990a). This paper (91-32) is published with approval of the Kentucky Agricultural Experiment Station.
* To whom correspondence should be addressed.
‡ University of Kentucky.
§ Present address: Department of Chemistry and Biochemistry, Utah State University, Logan, UT 84322-0300.
∥ Michigan State University.
⊥ University of Nebraska.

[1] Abbreviations: $C_1^+$ and $C_2^+$, photooxidizable radicals, tentatively associated with $Chl^+$ and $Car^+$, respectively; Car, carotenoid; Chl, chlorophyll; cyt *b*-559, cytochrome *b*-559; $D_1$ and $D_2$, homologous 32-kDa polypeptides which, as a dimer, form the PSII RC core; DCIP, 2,6-dichlorophenolindophenol; DCMU, 3-(3,4-dichlorophenyl)-1,1-dimethylurea; DPC, diphenylcarbazide; EPR, electron paramagnetic resonance; MES, 2-(*N*-morpholino)ethanesulfonic acid; $NH_2OH$-PSII, PSII membranes extracted with $NH_2OH$ to inactivate water oxidation; $P_{680}$, PSII primary electron donor chlorophyll; Pheo, pheophytin; PSII, photosystem II; $Q_A$ and $Q_B$, primary and secondary plastoquinone electron acceptors of PSII, respectively; RC, reaction center; $S_n$ (state), oxidation state of the WOC; WOC, water-oxidizing complex; $Y_Z$ and $Y_D$, redox-active tyrosines-161 and -160, respectively, of the $D_1$ and $D_2$ RC polypeptides.

0006-2960/91/0430-7586$02.50/0 